# Supporting Information

## Sanchez et al. 10.1073/pnas.1719695115

### SI Text

**Data Sources.** We determine US ethanol biorefinery location and near-term production capacity based on data from the Renewable Fuels Association (1). Saline aquifer storage capacity and location are derived from v1502 of the National Carbon Sequestration database (NATCARB) (2). We adopt existing pipeline rights of way as defined by the National Pipeline Mapping System for our candidate $CO_2$ transmission network (3, 4). We assume a 10% cost of capital and a 20-y project lifetime. We adjust capital costs of pipelines to 2014 using US Bureau of Labor Statistics cost indices and the costs of storage using the IHS Upstream Capital Cost Index.

**Calculation of Market Size and Carbon Intensity in California LCFS.** We estimate the market size and overall abatement that ethanol with CCS can provide in California through 2030 based on demand forecasts, fuel blending constraints, proposed standards, and lifecycle assessment. Specifically, we adapt California Air Resources Board (ARB) April 2015 assumptions about gasoline demand, growth of ethanol blending, and rates of improvement in carbon intensity of biofuels from the ARB's Illustrative Compliance Scenario for the LCFS (5). We assume that 2020–2025 trends assumed by ARB continue through 2030.

Calculating the quantity of abatement possible from ethanol with CCS requires knowledge of (*i*) potential market penetration, (*ii*) lifecycle carbon intensity of ethanol with CCS, and (*iii*) 2030 targets for the LCFS. First, we assume that all California ethanol demand can be met by ethanol with CCS. As discussed elsewhere in this paper, LCFS abatement credit prices will likely incentivize installation of CCS on existing biorefineries and can likely incentivize transport of ethanol to California from out-of-state producers. Nevertheless, we do not assume that low-carbon ethanol demand increases as a result of market forces. Second, we assume that adoption of CCS on ethanol can, on average, reduce its lifecycle carbon intensity by 32 $gCO_2$-eq/MJ as estimated elsewhere (6). As a result, we estimate that ethanol with CCS has a carbon intensity of 25 $gCO_2$-eq/MJ in 2030. Third, we evaluate three scenarios for 2030 carbon intensity targets in the LCFS: 10, 12, and 20% reduction from a 2010 baseline. California's 2017 Climate Change Scoping Plan examines 10, 18, and 25% reduction from a 2010 baseline by 2030.

In total, we estimate that biorefineries can contribute roughly 1.5 billion gallons/y of ethanol with CCS to the California market through 2030. While the supply of ethanol with CCS may be larger, other limitations, like fuel blending constraints, may prevent further supplies from being used for LCFS compliance. Depending on the 2030 target, annual abatement from this supply is between 7 and 8 $MtCO_2$/y in 2030. As California aims to reduce its total emissions by 40% from 1990 levels in 2030, ethanol CCS can contribute 4–5% to California's 2030 goal (7). As the total production capacity for ethanol with CCS from existing biorefineries is 15.8 billion gallons/y, remaining ethanol can be used to meet decarbonization goals in other jurisdictions outside California.

**International Context.** Our analysis—along with others—suggests that other countries could adopt CCS at ethanol biorefineries, likely at low costs. Globally, fermentation released 76 $MtCO_2$ in 2016 (8). Many regions producing ethanol, including Brazil, China, Canada, and the EU, are colocated with sedimentary basins suitable for geologic sequestration (9). Preliminary work suggests an overlap between sugarcane biorefineries and storage locations in Brazil, which produce 28 $MtCO_2$/y from fermentation (10, 11). Indeed, Brazil proposed a large-scale CCS demonstration at a sugarcane biorefinery in the state of Sao Paolo in 2010, which was abandoned due to a lack of domestic financial support. Policy support may be necessary to deploy CCS on ethanol in these countries.

**Discussion of Technological Readiness.** Deployment of CCS at biorefineries is technically mature. Capture, compression, dehydration, transportation, and sequestration of fermentation $CO_2$ streams use existing technologies already deployed at commercial scales in the United States (12–14). For instance, the largest compressor deployed in our analysis is a commercially available 3.8-MW unit (15). By comparison, the largest compressor at the Illinois industrial CCS project was 2.4 MW. Similarly, we assess pipeline costs using widely used X70 steel (16). Most importantly, we do not rely on widespread deployment of costly or unproven solvents, sorbents, or membranes for commercial-scale $CO_2$ capture (17).

**Determination of Storage Costs.** Saline aquifer storage capacity and location are derived from v1502 of the NATCARB (2). We evaluate only "assessed" geologic storage resources with meaningful values for thickness and in which $CO_2$ would exist as a dense liquid or supercritical fluid. Density of the injected $CO_2$ at reservoir conditions was estimated using a cubic equation of state with Peng–Robinson parameters (18). We assumed a 0.5 net-to-gross ratio to estimate net thickness of the reservoir from the reported total thickness. Estimated values were used where storage resources were missing depth, reservoir temperature or pressure, total dissolved solids content of the formation water, or porosity. Following this process, we found that 162,000 of the total 187,000 database entries, each of which represents a 10 × 10-km area in a storage reservoir, contained data sufficient to estimate storage cost. (In addition, we corrected for incorrectly formatted porosity values reported by two of the regional carbon sequestration partnerships.)

Using reservoir data from the NATCARB database, we then assess sequestration costs for each 10 × 10-km area in each storage resource, which include the cost of site characterization based on areal footprint, well drilling and completion, injection equipment, operating and maintenance costs, and ongoing monitoring and verification costs. This is based on methods in refs. 19 and 20. Specifically, we calculate the levelized cost of sequestration based on the following formula:

$$C_{seq}(\$/\text{ton}) = CRC \times \left(C_{well,D\&C} + C_{well,equip} + C_{well,O\&M}\right) \Big/ q_{well,max} + CRC \times C_{char}/q_{annual} + C_{mon},$$

where

$CRC$ = capital recovery factor,

$C_{well,D\&C}$ = cost of drilling and completion,

$C_{well,equip}$ = cost of well equipment,

$C_{well,O\&M}$ = cost of well operation and maintenance,

$q_{annual}$ = annual injection volume (at reservoir conditions),

$C_{char}$ = site characterization costs,

$C_{mon}$ = monitoring costs, and

$q_{well,\ max}$ = maximum well injection rate.

Costs are taken from ref. 20 and updated to 2014 US dollars (USDs) using the IHS Upstream Capital Cost Index. We assume that the maximum well injection rate is 1 $MtCO_2/y$. Characterization costs depend on the size of the aerial footprint. We apply an approximation for the maximum plume radius, $r_{max}$, from ref. 21:

$$C_{char}(\$) = C_{areal,char} \times \lambda_c \times q_{annual} \times t / (\phi \times b \times \lambda_w),$$

where

$C_{areal,char}$ = specific site characterization costs,

$q_{annual}$ = annual injection volume (at reservoir conditions),

$\lambda_c$ = phase mobility of $CO_2$(ratio of relative permeability to fluid viscosity),

$\lambda_w$ = phase mobility of brine,

t = period of injection,

$\phi$ = porosity, and

b = thickness of $CO_2$ layer.

The physical properties required to estimate the viscosity needed for the phase mobilities of $CO_2$ and brine were estimated using the correlations of Chung et al. (22) and Batzle and Wang (23), respectively. We assumed relative permeability end points of one for both $CO_2$ and brine. We include a fixed cost of \$52 million per site to account for development costs based on ref. 15. We assume a cost of monitoring, verification, and liability of \$0.19/$tCO_2$ (2014).

To reduce computational constraints, the gridded 10 × 10-km-resolution NATCARB data were then aggregated to 100 × 100-km grid cells while maintaining each unique aquifer layer as identified by resource, basin, and depth. However, this results in more than 39,000 individual layers and up to 445 layers per grid cell. To further reduce complexity, the mean injection cost for each resource is calculated and weighted by sequestration capacity. Thus, individual resources within each grid cell are represented by unique injection costs and capacities. The resulting dataset includes 2,216 unique resources within 436 grid cells with up to 23 resources per grid cell.

**Determination of Pipeline Costs.** We use the method and default assumptions outlined by McCoy and Rubin (24) to calculate the maximum mass flowrate for a nominal pipeline size (NPS) for a set pressure drop per unit length as provided in Table S1. Notably, we assume that commonly available X70 line pipe is used with a design factor of 0.72 (per the US Code of Federal Regulations) for the calculation of pipe wall thickness, and pressure drop is 35 kPa/km, which is well within the optimal range suggested by Knoope et al. (16).

We then used the model recommended by Knoope et al. (16) to calculate materials, labor, rights of way, and miscellaneous costs associated with pipeline construction. We convert the 2010 Euro costs presented therein to USD using the average 2010 exchange rate and then rebase the costs to 2014 USD using appropriate US Bureau of Labor Statistics cost indices.

**System Boundaries Used in Scenario Design.** We consider two credit scenarios: sequestration and abatement. Sequestration credits (dollars per $tCO_2$ sequestered) award credit based on the amount of $CO_2$ permanently sequestered, while abatement credits (dollars per $tCO_2$ abated) award credit based on the lifecycle amount of $CO_2$ abated via CCS. The amount of $CO_2$ abated is equal to that sequestered less the direct and indirect (i.e., electricity generation) emissions resulting from capture and compression. Average electricity grid emissions factors for North American Electric Reliability Corporation subregions were used to estimate the emissions from energy consumption for each biorefinery. Sequestration credits emulate existing CCS tax credits, which the current US Congress has proposed to strengthen, while abatement credits emulate tradeable climate policy instruments, such as credit prices in an LCFS, which reward lifecycle $CO_2$ emissions reductions. While ethanol producers may be able to claim both sequestration and abatement credits simultaneously, we study these credits independently. System boundaries for sequestration and abatement credits are shown in Fig. S3.

**Model Formulation.**

***Sets.*** Sets are as follows.

| | |
|---|---|
| *n* | Nodes |
| *d* | Pipeline diameter |
| *r* | Injection resource |
| Arc(*n*,*n*) | Potential pipeline rights-of-way connecting nodes |
| Sink(*n*,*r*) | Mapping set representing injection nodes |
| Facility(*n*) | Mapping set representing existing biorefineries |

***Parameters.*** Parameters are as follows.

| | |
|---|---|
| $CO_{2capt}(n)$ | $CO_2$ captured at each biorefinery (million tons per year) |
| $CO_{2abate}(n)$ | $CO_2$ abated at each biorefinery (million tons per year) |
| $LC_{capt}(n)$ | Levelized cost of $CO_2$ capture at each biorefinery (\$1,000 per million tons) |
| $LC_{inj}(n,r)$ | Levelized cost of $CO_2$ injection at each resource (\$1,000 per million tons) |
| $C_{diam}(d)$ | Capital cost of each pipeline diameter (\$1,000 per km) |
| $C_{pipe}(n,n,d)$ | Pipeline cost over life of project (\$1,000) |
| $Cap_{pipe}(d)$ | $CO_2$ capacity for each pipeline diameter (million tons per year) |
| $Cap_{stor}(n,r)$ | $CO_2$ capacity for each storage resource (million tons per project lifetime) |
| $Dist(n,n)$ | Distance of potential pipeline rights of way (kilometers) |

***Scalars.*** Scalars are as follows.

| | |
|---|---|
| $P_{capt}$ | Carbon price (\$1,000 per million tons captured) |
| $P_{abate}$ | Carbon price (\$1,000 per million tons abated) |
| Life | Project lifetime |
| $OM_{pipe}$ | Pipeline fixed operation and maintenance (percentage of capital cost) |
| *CRF* | Capital recovery factor |
| $C_{site}$ | Fixed site characterization cost (\$1,000 per project) |

***Variables.*** Variables are as follows.

| | |
|---|---|
| Cost | Total cost over project lifetime (\$1,000) |
| $x(n,n)$ | Flow over arc (million tons per year) |
| $y(n,n,d)$ | Usage of arc (binary) |
| $a(n,r)$ | $CO_2$ stored at node *n* and resource *r* (million tons per project lifetime) |
| $f(n,r)$ | Usage of storage resource (binary) |
| $c(n)$ | Adoption of CCS at biorefinery at node *n* (binary) |

***Equations.*** The objective was to minimize cost over project lifetime. For abatement credit scenarios,

$$\sum_{n\in\text{facility}} c(n)\times\text{life}\times\left[\left(CO2_{\text{capt}}(n)\times LC_{\text{capt}}(n)\right)-\left(CO2_{\text{abate}}(n)\times P_{\text{abate}}\right)\right]+\sum_{n,r\in\text{sink}}\left[f(n,r)\times C_{\text{site}}+a(n,r)\times LC_{\text{inj}}(n,r)\right]+\sum_{n,n\in\text{arc}}\sum_{d}C_{\text{pipe}}(n,n,d)\times y(n,n,d).$$

For sequestration credit scenarios,

$$\sum_{n\in\text{facility}} c(n)\times\text{life}\times CO2_{\text{capt}}(n)\times\left[LC_{\text{capt}}(n)-P_{\text{capt}}\right]+\sum_{n,r\in\text{sink}}\left[f(n,r)\times C_{\text{site}}+a(n,r)\times LC_{\text{inj}}(n,r)\right]+\sum_{n,n\in\text{arc}}\sum_{d}C_{\text{pipe}}(n,n,d)\times y(n,n,d)$$

subject to

$$\sum_{r}a(n,r)=c(n)\times CO2_{\text{capt}}(n)\times\text{life}+\sum_{\text{arc}(m,n)}x(m,n)\times\text{life}-\sum_{\text{arc}(n,m)}x(n,m)\times\text{life}\quad\text{(flow conservation)},$$

$$a(n,r)\le Cap_{\text{stor}}(n,r)\times f(n,r)\quad\text{(storage capacity constraint)},$$

$$x(n,n)\le\sum_{d}y(n,n,d)\times Cap_{\text{pipe}}(d)\ \text{(pipeline capacity constraint)},$$

$$\sum_{d}y(n,n,d)\le 1\quad\text{(one pipeline per corridor)},$$

$$\sum_{n\in\text{facility}}(n)\times CO2_{\text{capt}}(n)=\sum_{n,r\in\text{sink}}\frac{a(n,r)}{\text{life}}\quad(\text{CO}_2\text{ capture/storage equivalency}),$$

where

$$C_{\text{pipe}}(n,n,d)=\left[C_{\text{diam}}(d)\times Dist(n,n)\right]\times\left[CRF+OM_{\text{pipe}}\right]\times\text{life}.$$


1. Renewable Fuels Association (2015) Ethanol biorefinery locations. Available at www.ethanolrfa.org/resources/biorefinery-locations/. Accessed October 6, 2016.
2. NATCARB (2015) Energy data exchange (EDX). Available at https://edx.netl.doe.gov/group/natcarb. Accessed May 5, 2017.
3. US Department of Transportation (2010) National Pipeline Mapping System. Available at https://www.npms.phmsa.dot.gov/. Accessed May 5, 2017.
4. Johnson NAC (2012) Detailed spatial modeling of coal-based hydrogen infrastructure deployment with carbon capture and storage: Methods, implications, and insights. Available at https://search.proquest.com/openview/32859dcc9dbeac35796e57c8a8abf73e/1?pq-origsite=gscholar&cbl=18750&diss=y. Accessed May 5, 2017.
5. California Air Resources Board (2015) Low carbon fuel standard. Available at https://www.arb.ca.gov/regact/2015/lcfs2015/lcfs2015.htm. Accessed November 4, 2017.
6. McCoy S (2016) Reducing lifecycle biofuel emissions with CCS. Available at https://www.cslforum.org/cslf/sites/default/files/documents/tokyo2016/McCoy-BiofuelsCCS-TG-Tokyo1016.pdf. Accessed September 3, 2017.
7. California Air Resources Board (2017) AB 32 Scoping plan. Available at https://www.arb.ca.gov/cc/scopingplan/scopingplan.htm?utm_medium=email&utm_source=govdelivery. Accessed November 4, 2017.
8. World Fuel Ethanol Production (2015) Renewable fuels association. Available at www.ethanolrfa.org/resources/industry/statistics/. Accessed July 14, 2017.
9. Bradshaw J, Dance T (2005) *Mapping Geological Storage Prospectivity of CO2 for the World's Sedimentary Basins and Regional Source to Sink Matching*. Seventh International Conference on Greenhouse Gas Control Technologies (Elsevier, Amsterdam). Available at https://inis.iaea.org/search/search.aspx?orig_q=RN:38065576. Accessed July 14, 2017.
10. Moreira JR, Romeiro V, Fuss S, Kraxner F, Pacca SA (2016) BECCS potential in Brazil: Achieving negative emissions in ethanol and electricity production based on sugar cane bagasse and other residues. *Appl Energy* 179:55–63.
11. Rockett GC, Machado CX, Ketzer JMM, Centeno CI (2011) The CARBMAP project: Matching CO2 sources and geological sinks in Brazil using geographic information system. *Energy Procedia* 4:2764–2771.
12. Greenberg SE, McKaskle R (2016) *Insights into Cost of CCS Gained from the Illinois Basin-Decatur Project* (Carbon Sequestration Leadership Forum, Washington, DC).
13. Finley RJ (2014) An overview of the Illinois Basin–Decatur project. *Greenh Gases Sci Technol* 4:571–579.
14. Wallace M, Kuuskraa VA (2016) *Near-Term Projections of CO2 Utilization for Enhanced Oil Recovery* (Natl Energy Technology Lab, Pittsburgh, PA).
15. McCollum DL, Ogden JM (2006) Techno-economic models for carbon dioxide compression, transport, and storage & correlations for estimating carbon dioxide density and viscosity (Institute of Transportation Studies). Available at https://cloudfront.escholarship.org/dist/prd/content/qt1zg00532/qt1zg00532.pdf. Accessed May 5, 2017.
16. Knoope MMJ, Guijt W, Ramírez A, Faaij APC (2014) Improved cost models for optimizing CO2 pipeline configuration for point-to-point pipelines and simple networks. *Int J Greenh Gas Control* 22:25–46.
17. Boot-Handford ME, et al. (2013) Carbon capture and storage update. *Energy Environ Sci* 7:130–189.
18. Peng D, Robinson DB (1976) New 2-constant equation of state. *Ind Eng Chem Fundam* 15:59–64.
19. Ogden J, Johnson N (2010) Techno-economic analysis and modeling of carbon dioxide (CO2) capture and storage (CCS) technologies. *Developments and Innovation in Carbon Dioxide (CO2) Capture and Storage Technology*, Carbon Dioxide (CO2) Capture, Transport, and Industrial Applications, ed Maroto-Valer M (Woodhead Publ, Sawston, Cambridge, United Kingdom), Vol 1, pp 27–63.
20. McCoy ST (2008) *The Economics of CO2 Transport by Pipeline and Storage in Saline Aquifers and Oil Reservoirs* (Carnegie Mellon Univ, Pittsburgh, PA).
21. Nordbotten JM, Celia MA, Bachu S (2005) Injection and storage of CO2 in deep saline aquifers: Analytical solution for CO2 plume evolution during injection. *Transp Porous Media* 58:339–360.
22. Chung TH, Ajlan M, Lee LL, Starling KE (1988) Generalized multiparameter correlation for nonpolar and polar fluid transport properties. *Ind Eng Chem Res* 27:671–679.
23. Batzle M, Wang Z (1992) Seismic properties of pore fluids. *Geophysics* 57:1396–1408.
24. McCoy ST, Rubin ES (2008) An engineering-economic model of pipeline transport of CO2 with application to carbon capture and storage. *Int J Greenh Gas Control* 2:219–229.

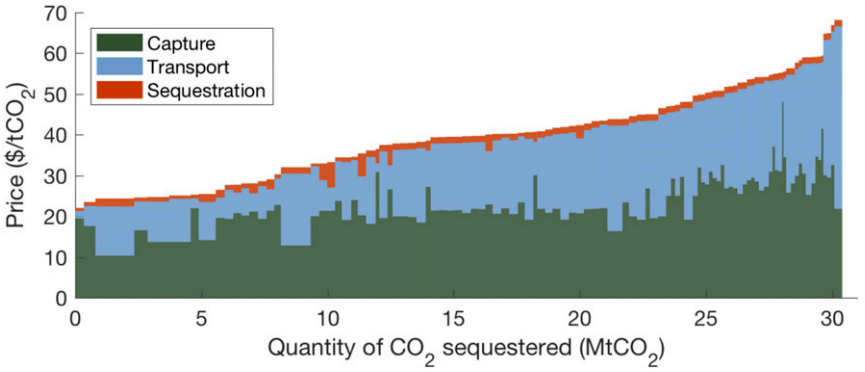


**Fig. S1.** Optimal supply curve for a $CO_2$ sequestration credit of \$60/t$CO_2$ reported at the facility level.

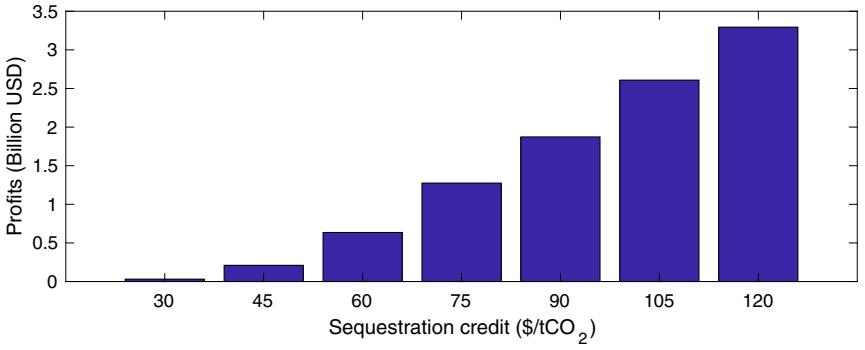


**Fig. S2.** Annual producer profits across sequestration scenarios.

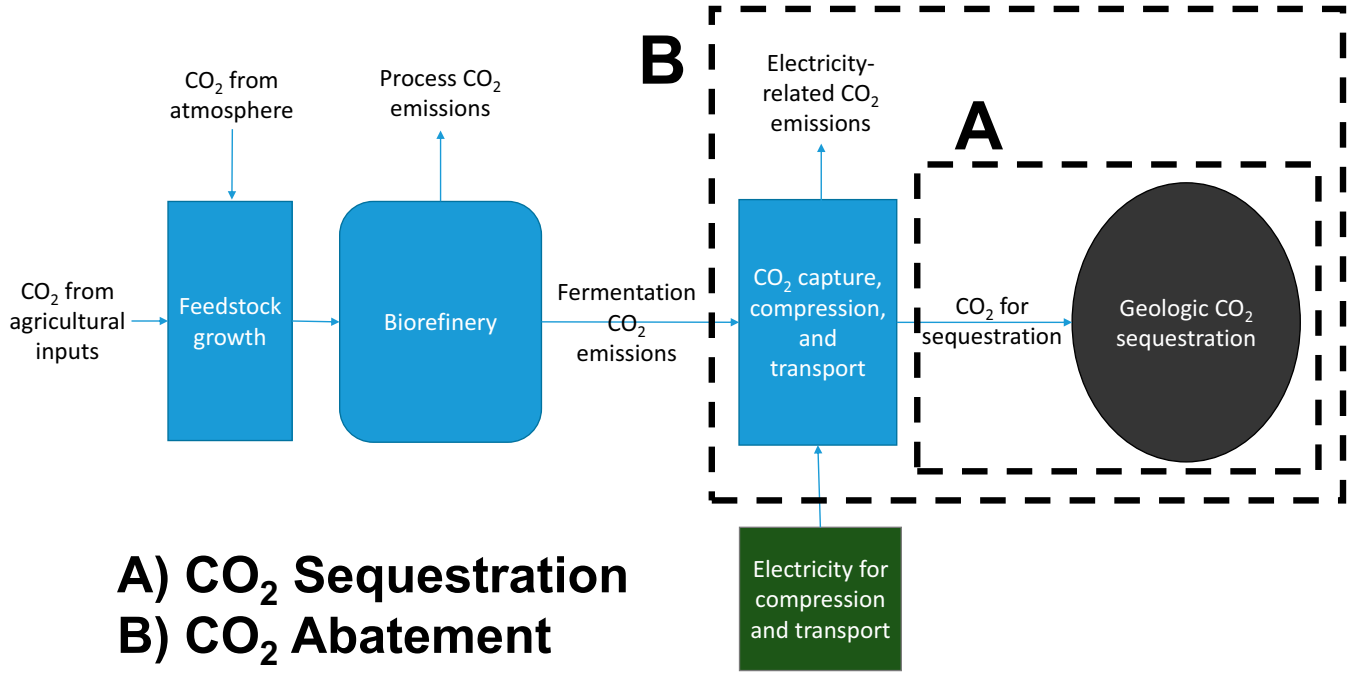


**Fig. S3.** System boundaries for sequestration (*A*) and abatement (*B*) credits. Sequestration credit scenarios award credit based on the amount of $CO_2$ permanently sequestered, while abatement credit scenarios award credit based on the lifecycle amount of $CO_2$ abated via CCS, including emissions from capture and compression.

**Table S1. Pipeline costs for each NPS considered in the optimization**

| NPS | Pipe o.d. (inches) | Pipe wall (inches) | Maximum flow (kt/y) | Material mass (kg/m) | Material cost (USD/m) | Labor cost (USD/m) | Right-of-way cost (USD/m) | Miscellaneous (USD/m) | Total (2014 USD/km) |
|---|---|---|---|---|---|---|---|---|---|
| 3 | 3.500 | 0.140 | 89 | 7.532 | $16.90 | $99.87 | $10.20 | $29.19 | $156,167 |
| 4 | 4.500 | 0.140 | 181 | 9.774 | $21.93 | $128.40 | $13.12 | $37.58 | $201,038 |
| 6 | 6.626 | 0.185 | 509 | 19.104 | $42.86 | $189.07 | $19.32 | $57.98 | $309,233 |
| 8 | 8.626 | 0.229 | 1,022 | 30.825 | $69.16 | $246.14 | $25.15 | $78.82 | $419,273 |
| 10 | 10.752 | 0.276 | 1826 | 46.308 | $103.90 | $306.80 | $31.35 | $102.68 | $544,727 |
| 14 | 14.000 | 0.348 | 3,650 | 75.981 | $170.47 | $399.48 | $40.82 | $142.49 | $753,266 |
| 18 | 18.000 | 0.436 | 7,045 | 122.518 | $274.89 | $513.62 | $52.48 | $197.13 | $1,038,117 |
| 22 | 22.000 | 0.524 | 11,898 | 180.087 | $404.05 | $627.76 | $64.14 | $257.95 | $1,353,907 |
| 26 | 26.000 | 0.612 | 18,393 | 248.687 | $557.97 | $741.90 | $75.81 | $324.97 | $1,700,636 |
| 30 | 30.000 | 0.700 | 26,698 | 328.319 | $736.63 | $856.03 | $87.47 | $398.17 | $2,078,304 |